Bed Agglomeration Characteristics and Mechanisms during Gasification and Combustion of Biomass Fuels

ARTICLE *in* ENERGY & FUELS · JUNE 2005

Impact Factor: 2.79 · DOI: 10.1021/ef040093w

3 AUTHORS:

Marcus Öhman
Luleå University of Technology
86 PUBLICATIONS **1,987** CITATIONS
SEE PROFILE

Linda Pommer
Umeå University
23 PUBLICATIONS **374** CITATIONS
SEE PROFILE

Anders Nordin
Umeå University
66 PUBLICATIONS **1,713** CITATIONS
SEE PROFILE

Article

Bed Agglomeration Characteristics and Mechanisms during Gasification and Combustion of Biomass Fuels

Marcus hman, Linda Pommer, and Anders Nordin

Energy Fuels, **2005**, 19 (4), 1742-1748• DOI: 10.1021/ef040093w • Publication Date (Web): 07 June 2005

Bed Agglomeration Characteristics and Mechanisms during Gasification and Combustion of Biomass Fuels

Marcus Öhman,* Linda Pommer, and Anders Nordin

Energy Technology and Thermal Process Chemistry, Umeå University, S-901 87 Umeå, Sweden

Received November 30, 2004. Revised Manuscript Received April 18, 2005

Controlled agglomeration tests, using six representative biomass fuels (bark, Lucerne, reed canary grass, bagasse, olive flesh, and cane trash) were performed in a bench-scale fluidized bed (5 kW) during both gasification and combustion conditions. The resulting bed materials were analyzed using scanning electron microscopy/energy-dispersive spectroscopy (SEM/EDS), and chemical equilibrium calculations were performed to facilitate the interpretation of the experimental findings. Layers of fuel-ash-derived compounds were built up on the bed particles during processing of all studied fuels. The accumulated material was determined to consist of two layers: (i) an inner thicker and more homogeneous layer that consisted of mainly K−Ca-silicates and (ii) a thinner, particle-rich outer layer. For all fuels except Lucerne, no major differences in bed agglomeration tendencies or bed particle layer characteristics could be detected between gasification and combustion, which suggested no major difference in layer formation processes or bed agglomeration mechanisms between the two different operational modes. Thus, initial silicate layer formation followed by subsequent viscous flow sintering and agglomeration was identified as the bed agglomeration process in all cases except during the combustion of Lucerne. For combustion of the relatively sulfur-rich Lucerne fuel, the agglomeration was induced by a salt melt where the bed material particles were directly glued together by a separate ash-particle-derived melt.

Introduction

Ash-related operating problems, such as slagging and fouling, have been reported extensively in the literature for most conventional combustion technologies. Because of the inherent advantages of low process temperatures, isothermal operating conditions, and fuel flexibility, fluidized bed technologies have been found to be the most suitable approach in converting a wide range of biomass fuels into energy. The bio-syngas produced from gasification of biomass may be used to produce power, liquid fuels, and chemicals or to replace petroleum oils or gases in industrial furnaces. However, biomass fuels contain relatively large amounts of alkali metals and it is well-known that high alkali-metal contents increase the agglomeration tendency of fluidized beds. Total defluidization due to agglomeration leads to severe unscheduled shutdowns and high operational and maintenance costs. Although bed agglomeration during gasification[1−8] and combustion[9−20] of biomass has been reported frequently, the responsible chemical mechanisms are far from being carefully elucidated.

* Author to whom correspondence should be addressed. Telephone: +46 90 7866324. Fax: +46 90 7869195. E-mail address: marcus.ohman@chem.umu.se.

(1) Bitowft, B. K.; Bjerle I. *Energy Biomass Wastes* **1998**, *11*, 511−529.
(2) Ergudenler, A.; Ghaly, A. E. *Bioresour. Technol.* **1993**, *43*, 259−268.
(3) Ergudenler, A.; Ghaly, A. E. *Biomass Bioenergy* **1993**, *4*, 135−147.
(4) Padban, N.; Kiuru, S.; Hallgren, A. L. *Prepr. Pap.—Am. Chem. Soc. Div. Fuel Chem.* **1995**, *40*, 743−747.
(5) Moilanen, A.; Kurkela, E.; Laatikainen-Luntama, J. *Proc. Eng. Found. Conf. Miner. Matter Fuels* **1997**, 555−567.
(6) Natarajan, E.; Öhman, M.; Gabra, M.; Nordin, A.; Liliedahl, T.; Rao, A. N. *Biomass Bioenergy* **1998**, *15*, 163−169.
(7) Arvelakis, S.; Gehrmann, H.; Beckmann, M.; Koukios, E. G. *Biomass Bioenergy* **2002**, *22*, 55−69.
(8) Zevenhoven-Onderwater, M.; Backman, R.; Skrifvars, B.-J.; Hupa, M.; Liliendahl, T.; Rosén, C.; Sjöström, K.; Engvall, K.; Hallgren, A. *Fuel* **2001**, *80*, 1503−1512.
(9) Salour, D.; Jenkins, B. M.; Vafaei, M.; Kayhanian, M. *Biomass Bioenergy* **1993**, *4*, 117−133.
(10) Nordin, A.; Öhman, M.; Skrifvars, B.-J.; Hupa, M. In *Applications of Advanced Technology to Ash-Related Problems in Boilers*; Baxter, L., DeSollar, R., Eds.; Plenum Press: New York, 1996; pp 353−366.
(11) Lin, W.; Krusholm, G.; Dam-Johansen, K.; Musahl, E.; Bank, L. *Proc. Int. Conf. Fluid. Bed Combust.* **1997**, *14th* (2), 831−837.
(12) Olofsson, G.; Ye, Z.; Bjerle, I.; Andersson, A. *Ind. Eng. Chem. Res.* **2002**, *41*, 2888−2894.
(13) Lin, W.; Dam-Johansen, K.; Frandsen, F. *Chem. Eng. J.* **2003**, *96*, 171−185.
(14) Öhman, M.; Nordin, A.; Skrifvars, B.-J.; Backman, R.; Hupa, M. *Energy Fuels* **2000**, *14*, 169−178.
(15) Latva-Somppi, J.; Kauppinen, E. I.; Valmari, T.; Ahonen, P.; Burav, A. S.; Kodas, T. T.; Johanson, B. *Fuel Process Technol.* **1998**, *54*, 79−94.
(16) Latva-Somppi, J.; Kurkela, J.; Tapper, U.; Kauppinen, E. I.; Jokiniemi, J. K.; Johanson, B. In *Proceedings of the International Conference on Ash Behavior Control in Energy Conversion Systems*; 1998; pp 119−126.
(17) Nuutinen, L. H.; Tiainen, M. S.; Virtanen, M. E.; Enestam, S. H.; Laitinen, R. S. *Energy Fuels* **2004**, *18*, 127−139.
(18) Brus, E. Thesis, Umeå University, Umeå, Sweden, 2004. (ISBN 91-7305-676-6.)
(19) Brus, E.; Öhman, M.; Nordin, A.; Boström, D.; Hedman, H.; Eklund, A. *Energy Fuels* **2004**, *18*, 1187−1193.
(20) Brus, E.; Öhman, M.; Nordin, A.; Skrifvars, B. J.; Backman, R. *IFRF Combust. J.* **2003**, Article Number 200302. (ISSN 1562−479X.)

10.1021/ef040093w CCC: $30.25
Published on Web 06/07/2005

Table 1. Fuel and Bed Material Characteristics

	Lucerne	bagasse	cane-trash	reed canary grass	bark	olive flesh	bed material
dry substance[a]	92.1	91.5	90.8	90.5	90.6	85.6	
ash (wt %, d.b.)	8.5	6.8	8.0	5.7	3.0	9.9	
Na (wt %)[b]	0.56	0.52	0.44	0.91	1.2	1.3	0.030
K (wt %)[b]	22	3.6	12	3.0	6.4	15	0.050
Ca (wt %)[b]	20	3.1	3.7	3.9	28	13	0.088
Mg (wt %)[b]	2.0	1.6	1.8	0.76	2.4	7.5	0.078
Al (wt %)[b]	0.22	4.6	1.7	0.76	1.2	1.9	0.096
Fe (wt %)[b]	0.22	3.9	1.4	0.60	2.7	3.0	0.086
Si (wt %)[b]	1.8	36	27	36	6.8	17	46
S (wt %)[b]	1.9	0.29	0.25	1.8	1.0	1.4	
Cl (wt %)[b]	4.1	0.88	2.5	0.53	0.33	1.5	
P (wt %)[b]	3.6	0.41	0.92	0.91	1.2	1.8	<0.0052

[a] Weight percent of fuel. [b] Weight percent of ash.

Two different routes for agglomeration have been suggested in the literature,[18,21] and these routes are referred to as (i) "melt-induced" agglomeration, for bed materials directly glued together by a separate ash-derived melt phase, and (ii) "coating-induced" agglomeration, for the sequential process of coating formation on the bed particles, followed by adhesion and agglomeration. Coating-induced agglomeration has been suggested to be the main route for agglomeration during fluidized bed combustion of biomass fuel,[18,21] where the coatings may consist of compounds with low melting temperatures, which can result in agglomeration of the bed material[11,14] or, in the worst case, defluidization of the bed. The coating formation and characteristics has been studied in detail during combustion of biomass fuels in both bench-scale[14,18,19] and full-scale processes.[16,17,20] Bed particle coatings from biomass combustion have been shown to consist of multiple layers,[17,19,22] and the composition of these layers is controlled by both the fuel and the composition of the bed material.[17,19,22] The composition of the inner layer is dependent both on the fuel characteristics and the composition of the bed material, whereas the composition of the outer layers is dependent primarily on the fuel characteristics.[17,19,22] The inner layer is reported to be similar to that of the adhesive materials in agglomerates containing increased levels of K−Ca-silicates with varying levels of other elements.[17,19] During combustion of typical wood fuels, attack (reaction) and diffusion by calcium into the quartz resulting in low-melting silicates (also including minor amounts of, for example, potassium) with subsequent viscous flow sintering has been identified to be the dominating agglomeration mechanism.[18] For high-alkali-containing biomass fuels, direct attack by potassium compounds in the gas or aerosol phase, resulting in low-melting potassium silicates with subsequent viscous flow sintering, has been identified to be the dominating agglomeration mechanism.[18]

However, there is still lack of detailed information about the bed particle layer formation/bed agglomeration process during gasification of biomass. This inspired us to study the bed particle layer formation and characteristics during gasification more closely. Therefore, the objectives of the present work were (i) to elucidate the bed agglomeration process during biomass gasification, and (ii) determine if there are any potential differences in bed agglomeration mechanisms and agglomeration tendencies between gasification and combustion conditions. Controlled agglomeration experiments of several representative biomass fuels in both gasification and combustion atmospheres were performed. In addition, chemical equilibrium model calculations were used to interpret the experimental findings.

Experimental Section

Fuels and Bed Material. The biomass fuels chosen for the study were bark (as a typical wood fuel), reed canary grass, Lucerne, olive flesh, cane trash, and bagasse. These fuels were selected based on a principal component analysis (PCA)[23] where a biomass fuel database[24] that contained more than 300 analyzed samples of different biomass fuels, thus covering most of the typical variations in the ash composition of biomass fuels, was used. The selected fuels represent different classes of biomass fuels and their fuel-ash characteristics are shown in Table 1.

The fuels were pelletized to a diameter of 6−8 mm and a length of 5−10 mm and then were used for the controlled bed agglomeration tests.[25] The tendency to cause bed agglomeration in a sand bed was tested by determination of the characteristic critical agglomeration temperatures during both gasification and combustion conditions. The bed material used during each experiment was 540 g of normal quartz sand (see Table 1), initially sieved to a size range of 200−250 μm. The sand contained >98% SiO_2 and only small amounts of mineral impurities.

Controlled Fluidized Bed Agglomeration Tests. The controlled fluidized bed agglomeration (CFBA) method has previously been described more fully by Öhman and Nordin,[25] and only a brief description is given here. The bench-scale reactor (5 kW) is constructed from stainless steel and has dimensions of 2 m high and 100 and 200 mm in bed and freeboard diameters, respectively. A schematic diagram of the reactor is given in Figure 1. To obtain isothermal conditions in the bed, and to minimize the significant influence of cold walls in such a small-scale unit, the reactor is equipped with electrical wall heating elements, equalizing the wall and bed temperatures.

In the combustion experiments, the agglomeration tests were initiated by loading of the bed with a certain ash to bed material ratio, under normal fluidized bed combustion (FBC) conditions. The excess oxygen concentration was controlled to $6\%_{dry}$. A fluidization velocity of four times the minimum fluidization velocity was used, and the bed temperature was maintained at 760 °C for all fuels except Lucerne, in agreement with a previously determined standard procedure.[25] To avoid

(21) Visser, H. J. M.; van Lith, S.; Kiel, J. H. A. In *12th European Conference on Biomass for Energy, Industry and Climate Protection*, Vol. 1; 2002; pp 585−588.
(22) Nuutinen, L. H.; Tiainen, M. S.; Virtanen, M. E.; Laitinen, R. S. *Proc. Int. Conf. Fluid. Bed Combust.* **2003**, *17th*.
(23) Wold, S. *Technometrics* **1978**, *20*, 397.
(24) Nordin, A. *Biomass Bioenergy* **1994**, *6*, 339−347.
(25) Öhman, M.; Nordin, A. *Energy Fuels* **1998**, *12*, 90−94.

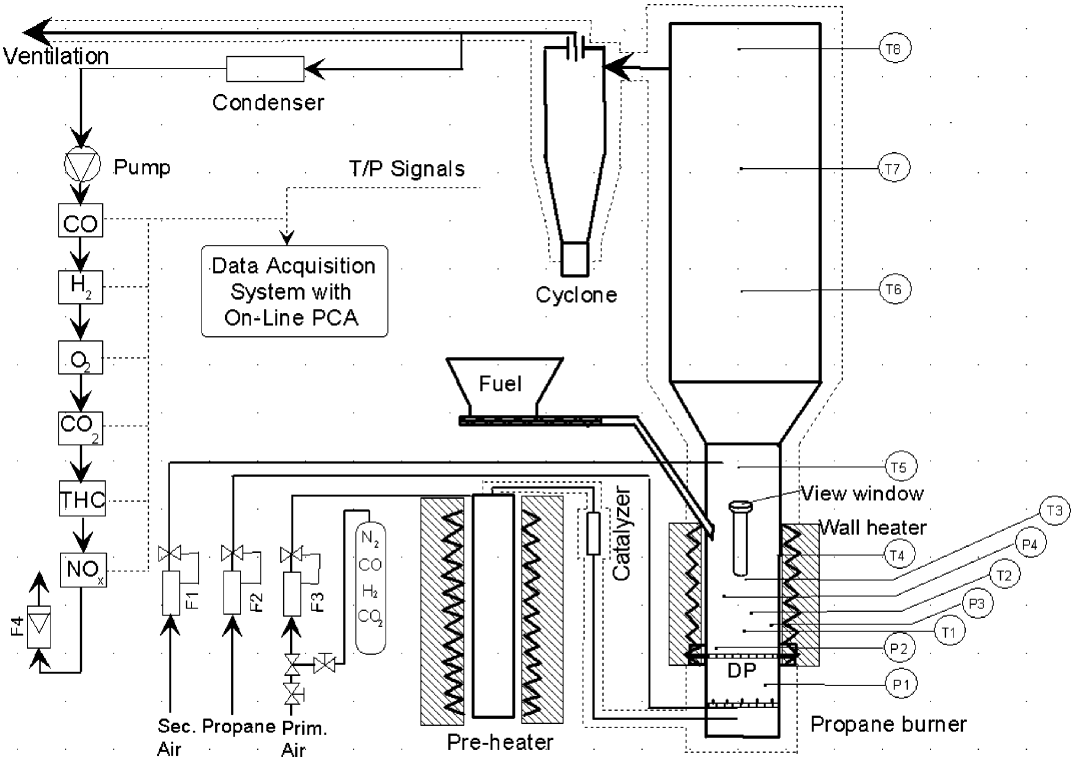

Figure 1. Illustration of the bench-scale fluidized bed reactor. Legend: P1−P4, differential bed pressures; T1−T8, thermocouples; F1−F3, mass-flow controllers; and DP, distributor plate.

Table 2. Elements and Solution Models Used in the Chemical Equilibrium Model Calculations[a]

elements	C, H, O, N, S, Cl, P, K, Na, Ca, Mg, Fe, Mn, Si, Al
solution models	
slag	? slag-liquid (MgO, FeO, MnO, Na_2O, SiO_2, CaO, K_2O)
salt	A salt-liquid (NaCl, KCl, NaOH, Na_2SO_4, K_2SO_4, Na_2CO_3, K_2CO_3)
(Ca, Mg)	liquid-K,Ca/CO_3,SO_4 (−LCSO)
	solid−K,Ca/CO_3,SO_4 (−SCSO)
	solid-Ca(SO_4),Mg(SO_4) (−SCMO)
	liquid-Ca,Mg,Na/(SO_4) (−LSUL)
	solid-Ca,Mg,Na/(SO_4) (−SSUL)

[a] The designations of the solution models are taken from the software program FactSage v. 5.2.

agglomeration during the ashing procedure for this fuel, a bed temperature of 600 °C was used. At an ash amount corresponding to a theoretical value of ∼20 wt % ash in the bed, the fuel feeding was stopped and the operation was switched to external heating. Previously initial runs have shown that 1.5% of ash in the bed is sufficient for agglomeration to occur.[25] The bed was then isothermally heated at a rate of 3 °C/min by means of an external primary air heater and wall heaters in a homogeneous and controlled manner until bed agglomeration was achieved. To maintain a combustion atmosphere in the bed during the external heating phase, propane was mixed with primary air in a chamber prior to the air distributor.

In the gasification experiments, the agglomeration tests were initiated by loading the bed with an ash to bed material ratio of ∼20 wt % ash in the bed (theoretical), under normal fluidized bed gasification (FBG) conditions, i.e., the fuel was gasified in the bed with 35% of stoichiometric air. The same bed temperature and fluidization velocity as in the combustion experiments were used. When the predetermined ash-to-bed ratio was achieved, the fuel feeding was stopped and a similar gasification atmosphere was established in the bed. To achieve this, a gas mixture that contained CO, CO_2, H_2, and N_2 was passed through the primary air-heater and a platinum catalyst before entering the bed. The composition of this gas mixture was estimated from chemical equilibrium model calculations. To ensure that the desired gasification atmosphere was achieved, gas samples were collected before the distributor plate and analyzed via gas chromatography (GC-TDC). After the above procedure, the bed was heated, at a rate of 3 °C/min, to the point where it agglomerated. After the experiment, the bed was cooled in N_2.

Table 3. Initial Agglomeration Temperatures in Controlled Fluidized Bed Combustion and Gasification for the Different Fuels

	Initial Agglomeration Temperature (°C)	
	gasification	combustion
bark	930	980
Lucerne	840	660
reed canary grass	940−990	920−970
Bagasse	>1020	>1020
olive flesh	880	930
cane trash	840	880

The onset of bed agglomeration was determined by monitoring differential pressures and temperatures in the bed. The detection of initial bed particle cohesion was facilitated by PCA by considering all bed-related variables (three temperatures and four differential pressures) simultaneously. The results from a previous sensitivity analysis of the method showed the reproducibility of the bed agglomeration temperature to be ±5 °C (standard deviation).[25]

Scanning Electron Microscopy/Energy-Dispersive Spectroscopy (SEM/EDS) Analyses of Bed Material. The resulting bed samples were mounted in epoxy, cut by a diamond saw, and polished. The bed samples were then characterized using SEM/EDS, to determine the elemental

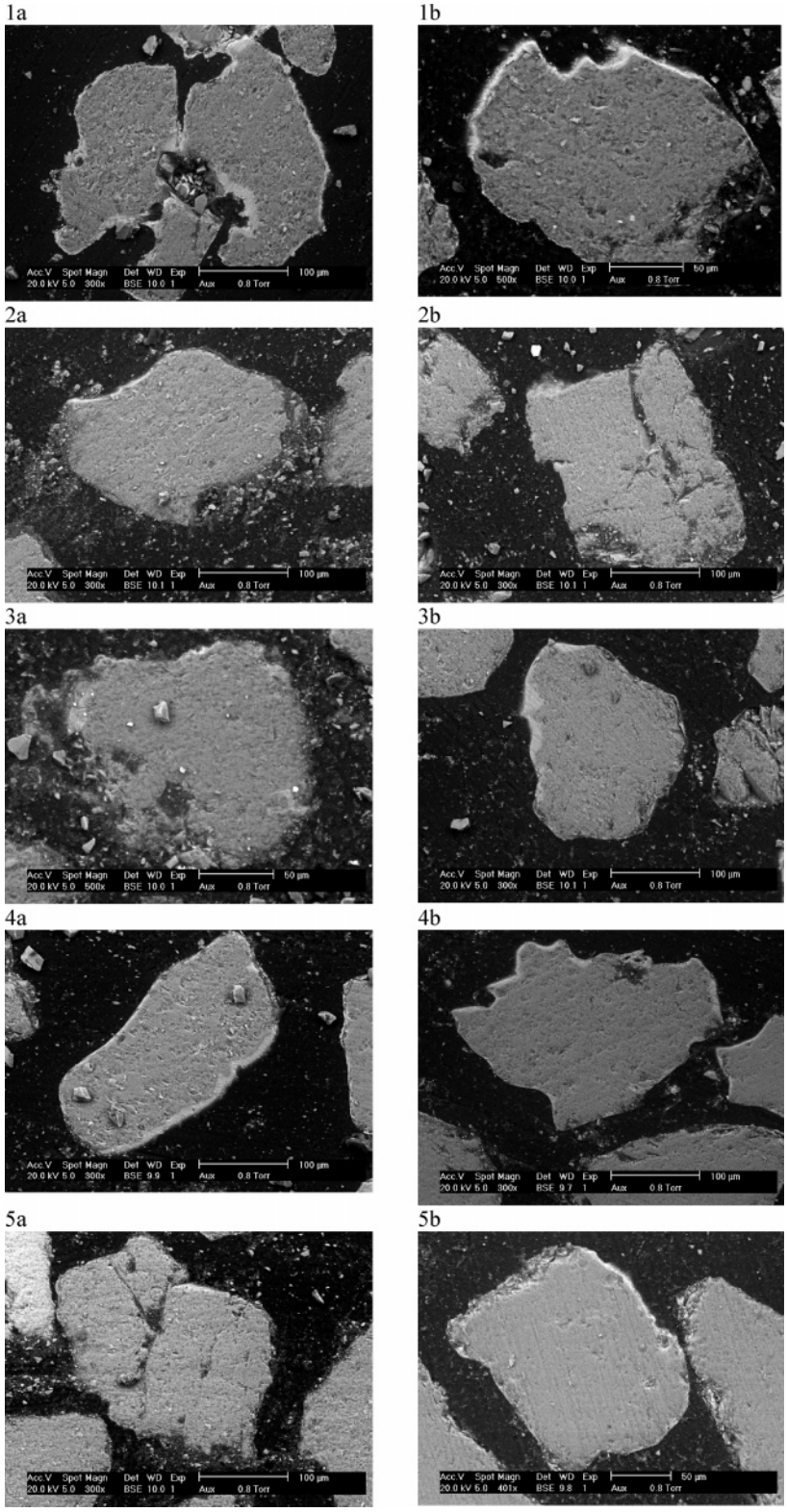

Figure 2. Bed particles from (a) combustion and (b) gasification: (1) bark, (2) cane trash, (3) Lucerne, (4) olive flesh, and (5) reed canary grass.

composition and to estimate the thickness of the formed bed particle layers. Several bed particles (3−5) from each bed sample were analyzed. The elemental composition of the inner layer was analyzed in several spots (3−5) for each bed particle. To avoid contributions from the bed material, special care was taken not to collect EDS data from spots close to the interface between the inner layer and the bed particle. Because of the too-thin outer layer of the bed particles, the elemental composition of this layer could not be measured with sufficient accuracy.

Chemical Equilibrium Model Calculations. To facilitate the interpretation of the experimental findings, chemical equilibrium model calculations were performed using the software program FactSage v. 5.2. The program uses the method of minimization of the total Gibbs free energy of the system. Thermodynamic data were taken from the Fact

database,[26] including all available stoichiometric data as well as the accompanying models for non-ideal solid and liquid solutions. Fuel compositions that are given in Table 1 were used. The calculations were performed using a global approach for atmospheric pressure (1 bar), and an air-to-fuel ratio (λ) of 1.6 and 0.35, corresponding to the combustion and gasification bench-scale experiments, respectively. Since previous work has shown that quartz sand reacts with ash-forming elements from the biomass fuel during combustion (forming an inner attack (reaction) layer consisting of silicates[18,19]), calculations where performed, assuming that some of the quartz bed particle, corresponding to the average thickness of the formed inner layers (~5 μm), participates in the chemical reaction. The calculations were conducted over a temperature range of 600−1100 °C.

Two separate liquid phases were assumed in the calculations, comprising the potentially coexisting oxide/silicate (slag) melt and an alkali-salt melt. Aluminum was excluded from the slag melt, because the melting temperatures for the fuel mixtures when aluminum was included were observed to be unexpectedly low; moreover, data for the $K_2O-Al_2O_3-SiO_2$ system is considered to be very approximate.[26] In addition, all relevant binary solid and liquid solutions with calcium and magnesium were included. The elements and solution models used in the calculations are shown in Table 2. From the calculations, the predicted amounts of melt and solid phases, as functions of temperature, could be extracted.

Results and Discussion

The resulting initial agglomeration temperatures from the CFBA tests are listed in Table 3. A marginal decrease in the initial agglomeration temperature was observed in gasification, compared to combustion when bark, olive flesh, or cane trash was used as fuel. Since bagasse had bed agglomeration temperatures above the maximum temperature for both these experiments (1020 °C), no differences in agglomeration temperatures could be determined for that fuel. No significant difference in bed agglomeration tendencies was detected for reed canary grass; however, for Lucerne, a major difference in agglomeration temperature (180 °C) between the two operational modes was detected, where the agglomeration temperature during gasification was markedly increased.

Typical illustrations of cross sections of the bed particle surfaces during both combustion and gasification are shown in Figure 2. Bed particle layers were formed both during gasification and combustion for all fuels. The accumulated material around the bed particles was often determined to consist of two layers during both combustion and gasification (Figure 3). The inner thicker layers were more homogeneous and the outer very thin layers were more particle-rich, in agreement with the results from full-scale combustion of biomass.[20] The layer thickness varied around the bed particles, as the layers formed on concave parts of the bed particle surface were considerable thicker than layers formed on convex parts. However, these layers could only be found on <10% of the bed particles produced during gasification and combustion of bagasse.

The total thickness of the formed layers was 2−8 μm during both combustion and gasification of bark, cane trash, and reed canary grass. These layers were formed on the majority, ~10%−30%, and only on 10% of the bed particles during both combustion and gasification of bark, cane trash, and reed canary grass, respectively. The initial rate of total layer formation, on the order of a few micrometers per day, were determined to be in general agreement with previous full-scale results during wood combustion.[20] The results from using olive flesh as fuel showed that the majority of the resulting bed particles were covered with layers of 4−20 μm in both combustion and gasification. For Lucerne, a major difference in layer characteristics could be found between gasification and combustion. During combustion, the bed particle layers were thin (1−3 μm) and particle-rich and only found on ~10% of the bed particles. Instead, the fuel-ash-derived material in the bed dominated as separate ash particles that consisted

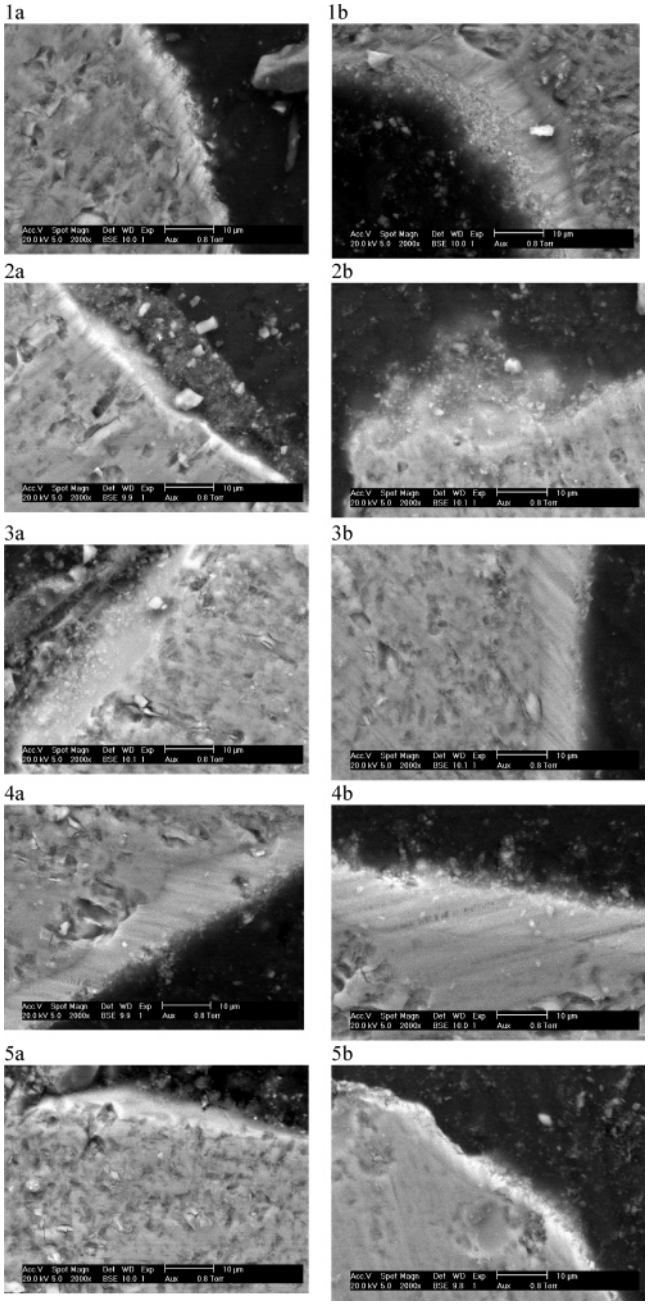

Figure 3. Illustration of typical bed particle cross sections from (a) combustion and (b) gasification: (1) bark, (2) cane trash, (3) Lucerne, (4) olive flesh, and (5) reed canary grass.

(26) Bale, C. W.; Pelton, A. D., FACT-database of FACT-Win version 3.05, CRCT École Polytechnique de Montréal, Quebec, Canada, 1999.

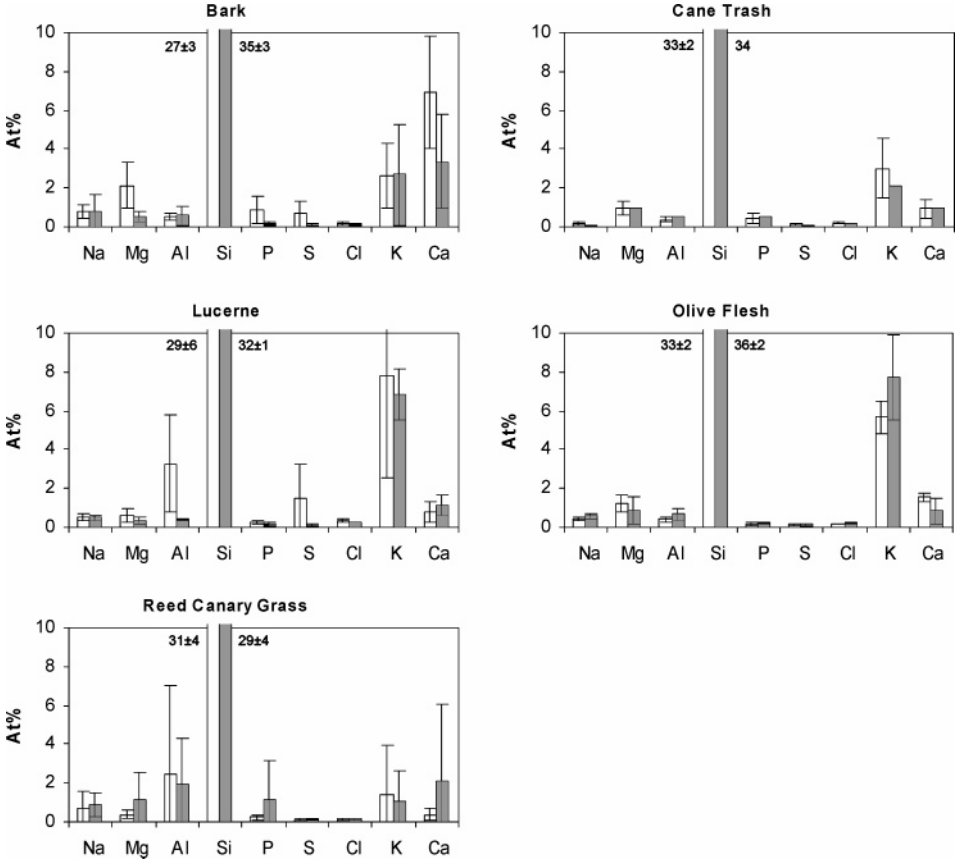

Figure 4. Elemental analyses of the formed inner layer around the bed particles during combustion (white bars) and gasification (gray bars) when using bark, cane trash, Lucerne, olive flesh, and reed canary grass as fuel.

of a salt matrix (Ca, K, S, P, CO_3, and some Cl).[10] During gasification, the layers were thick (3−20 μm) and more homogeneous, both in regard to structure and elemental composition (see Figure 4). These layers were found on the majority of the bed particles.

To quantify the elemental amounts found in the inner layers, a large number of EDS spot analyses were performed on each bed sample; the results are summarized in Figure 4. Each bar represents the average composition of several spot analyses taken from the inner bed particle layer or the neck formed between two bed particles. The results showed that the inner layer on the quartz bed particles consisted mainly of silicon, calcium, potassium, and oxygen during bark gasification and combustion, with only minor differences in elemental composition between the two operational modes. During combustion and gasification of cane trash and olive flesh, the inner layer consisted mainly of silicon, potassium, calcium, and oxygen. For reed canary grass, aluminum was also found as a major element in the inner layer. No significant differences in the elemental composition of the inner bed particle layer could be found for cane trash, olive flesh, and reed canary grass between the two operational modes. For Lucerne, the inner layer consisted mainly of silicon, potassium, and oxygen during gasification and silicon, potassium, sulfur, aluminum, and oxygen during combustion. Because of very thin layers during combustion, the measured elemental composition could be affected of the background level of the quartz particles. This could affect the measured silicon concentrations in these layers and thereby also the measured potassium, sulfur, and aluminum concentrations. Because the layers of the bed particles during the combustion and gasification of bagasse were too thin, these layers could not be analyzed.

For all studied fuels except Lucerne, the results from the equilibrium calculations (see Table 4) showed no major differences in the phases/solutions predicted to form between gasification and combustion. This agrees well with the present experience from the experiments that revealed no major differences in initial agglomeration temperatures or, bed particle layer characteristics between the two operational modes. As could be expected, an oxide/silicate (slag) melt is predicted to form for all fuels at higher temperatures, exact temperatures depending on fuel composition with only a minor effect on operational mode. The calculations did not show any major differences in regard to the dominant solid phases that are predicted to form in temperature range of 800−1100 °C for all fuels except Lucerne. In the case of Lucerne, the calculations predicted a salt melt rich in potassium, sulfur, and chlorine and solid K_2SO_4 to form during combustion, but not during gasification, where, instead, KCl reacting to form potassium silicates seems to be the preferred process. This is also thermochemically expected, as K_2SO_4 is not as stable as KCl in reducing atmospheres. The addition of K_2SO_4 to a salt system containing KCl is also expected to decrease the melting temperature. Therefore, the equilibrium calculations confirm the experimental experiences, which reveal a major difference in initial agglomeration temperatures and bed particle layer characteristics/formation during the combustion of Lucerne, compared to

Table 4. Phases/Solutions Predicted To Form during Combustion/Gasification in 775 °C, According to the Equilibrium Calculations[a]

	Bark		Olive Flesh		Lucerne[b]		Reed Canary Grass		Bagasse		Cane Trash	
phase/solution	comb.	gasificat.	comb.	gasificat.	comb.	gasificat.	comb.	gasificat.	comb.	gasificat.	comb.	gasificat.
ASalt−liquid					**; KCl, K_2CO_3, K_2SO_4							
?Slag−liquid								*; SiO_2, K_2O, Na_2O			**; SiO_2, K_2O, Na_2O	**; SiO_2, K_2O, Na_2O
$MgCaSiO_4$				**								
$MgCaSi_2O_6$			***	***			*		*	*	*	*
$MgCa_2Si_2O_7$	***	*										
$MgCa_3Si_2O_8$	*	***			**	**						
$Ca_3Fe_2Si_3O_{12}$	*											
$Ca_2FeSi_2O_7$		**			*							
$Na_2Ca_2Si_3O_9$	*	*	*	*	*	*						
$Na_2Ca_3Si_6O_{16}$			*				*	*				
$CaAl_2Si_2O_8$									*	*		
$NaAlSi_3O_8$									*	*		
$KAlSiO_4$					*	*						
$KAlSi_2O_6$	**	**	**	**			*	*	**	**	*	*
$CaSiO_3$	****	****										
Ca_2SiO_4						*						
$Ca_3Si_2O_7$					*							
K_2SiO_3						***						
$K_2Si_2O_5$	*	**	***	***	***	**						
$MgSiO_3$								*	*	*	*	*
Mg_2SiO_4			**	**								
$MnSiO_3$												*
$(FeO)_2(SiO_2)$								*		*		*
SiO_2							****	****	****	****	****	****
Fe_2O_3			*				*		*		*	
FeO				**								
Mn_2O_3	*						*				*	
$Ca_3(PO_4)_2$								*				
$Ca_5HO_{13}P_3$	*	*	*	*	**	**	*		*	*	*	*
K_2SO_4	*		*		**						*	
KCl					**	***						
FeS						*						

[a] Combustion/gasification temperature was 775 °C, unless noted otherwise. Legend in table is as follows: (****) dominant (>50 mol % of condensed phases); (***) subdominant (20−50 mol % of condensed phases); (**) minor (5−20 mol % of condensed phases); and (*) trace (<5 mol % of condensed phases). [b] Combustion/gasification temperature for Lucerne was 625 °C.

gasification. The difference in agglomeration temperature is most probably due to the presence of a salt melt during a relatively low temperature in combustion, which is not found during gasification. The major differences in bed particle layer thickness are probably due to a higher alkali concentration in the gas phase during gasification, leading to a relatively fast attack or chemical reaction with the quartz bed particle, in comparison, if potassium is present as K_2SO_4 particles, as was suggested during combustion.

Conclusions

The following conclusions can be drawn from the present work:

(1) Layers of fuel-ash-derived compounds were covering the bed particles during the gasification of all studied fuels. The accumulated material was determined to consist of two layers: a thicker and homogeneous inner layer, consisting of mainly K−Ca-silicates, and a thinner and particle-rich outer layer.

(2) For all fuels except Lucerne, no major differences in bed agglomeration tendencies or bed particle layer characteristics could be detected between gasification and combustion, which suggests that there is no major difference in layer formation processes or bed agglomeration mechanism between the two different operational modes. Thus, an initial silicate layer formation, followed by the subsequent viscous flow sintering and agglomeration, was the identified bed agglomeration process.

(3) For combustion of the relatively sulfur-rich Lucerne fuel, a salt melt induced agglomeration, where the bed materials were directly glued together by a separate ash-particle-derived melt, was identified as the responsible agglomeration process.

(4) Good agreements were generally obtained between the chemical equilibrium results and present experience from the experiments.

Acknowledgment. The financial support from the Swedish Energy Agency (STEM) is gratefully acknowledged.

EF040093W